PCCP

Accepted Manuscript

ROYAL SOCIETY OF CHEMISTRY

www.rsc.org/pccp

Phys. Chem. Chem. Phys. RSCPublishing

ARTICLE

Active Performance of Tetrahedral Groups to SHG Response: the Theoretical Interpretations of Ge/Si-Containing Borate crystals

Cite this: DOI: 10.1039/xoxxoooooox

Linping Li,[a b] Zhihua Yang,[b] Bing-Hua Lei,[b] Qingrong Kong,[b] Ming-Hsein Lee,[c] Bingbing Zhang,[b] Shilie Pan,[b] Jun Zhang*[a]

Received ooth January 2015,
Accepted ooth January 2015

DOI: 10.1039/xoxxoooooox

www.rsc.org/

As potential candidates for deep-UV nonlinear optical (NLO) crystals, borosilicates and borogermanates, which contain NLO-active groups such as B-O, Si-O and Ge-O, have fascinated many scientists' interests. The crystal structures, electronic structures and optical properties of seven borates in different B/R (R = Si, Ge) ratios have been studied by the DFT methods. Through the SHG-density, we find that besides the recognized contribution of π-conjugation configuration BO_3 to second harmonic generation (SHG), the tetrahedra have an un-negligible influence. This is because the non-bonding *p* orbitals of bridging oxygen in tetrahedra are observably closer to Fermi level than that in BO_3, which observed in the PDOS of $Rb_4Ge_3B_6O_{17}$ and $RbGeB_3O_7$. That conclusion would be very meaningful to understand the relationship between the crystal structure and nonlinear optical properties.

1. Introduction

With the development of laser micromaching, laser communication, and modern scientific instrument, the requirement for NLO crystals grows rapidly.[1-3] So far, commercialized optical crystals such as β-BaB_2O_4 (BBO),[4] LiB_3O_5 (LBO)[5] and $CsLiB_6O_{10}$ (CLBO)[6] have been applied, or potential candidates such as $Pb_{17}O_8Cl_{18}$ (POC),[7] $Ba_{23}Ga_8Sb_2S_{38}$,[8] $Ba_4B_{11}O_{20F}$ (BBOF),[2] $K_3B_6O_{10}Cl$ (KBOC)[9] emerge, while it is still challenging to get "wanted" NLO materials with the conditions satisfying "large SHG response", "laser damage threshold", or "short UV cut-off". According to the anionic group theory,[10] the main non-linearity of a crystal is the geometrical superposition of the microscopic second-order susceptibility of the constituent NLO-active anionic groups. Some well-known NLO-active anion groups, such as BO_3, CO_3, and NO_3 triangles with π-conjugation configuration,[11] MO_6 octahedra (M = Mo^{6+}, W^{6+}, Nb^{5+}, and V^{5+}) with d^0 transition metal ions,[12-14] and TO_n distorted polyhedra (T = Pb^{2+}, Bi^{3+}) with active lone pairs,[15, 16] have been explored as feasible NLO candidates. A crystal containing one more NLO active groups may possess a stronger NLO effect, typical examples are $Pb_2B_5O_9I$ with 13.5 × KDP[16] and $Pb_2(BO_3)(NO_3)$ with 9 × KDP[11]. However, BO_3 group possessing both wide transparency and large SHG effects still is one of the best structure units for deep-UV NLO materials.[17-19]

Ge/Si-contained alkaline, alkaline earth and rare earth metal borates are representative because of rich structures involved by combining groups of Ge/Si-O tetrahedra and B-O groups, such borates have fascinated many material scientists to study their optical properties due to their promising use in optical equipment.[20-24] Studies show that Ge/Si-containing borate crystals have the properties of deep-UV cut-off edge.[25] Up to now, a series of Ge/Si-containing borates have been synthesized, such as $Cs_2GeB_4O_9$[26], $Cs_2B_4SiO_9$[27] and $LaBGeO_5$[28], which are all potential in application for deep-UV second-order nonlinear-optical crystalline material based on their moderate SHG response and short cut-off edge under 200 nm.[26, 28-30] In addition, various frameworks built by B-O and R-O (R = Si, Ge) are potent factors to obtain excellent materials. Some investigators reported that the molar ratio of B/R can affect the structural type of such composite borate.[31] In B-riched R-containing borate with B/R > 1, the basic B-O units trend to condense into rings and then connect with RO_4, such as $RbGeB_3O_7$[20] with a B/Ge ratio of 3/1 and $Rb_2GeB_4O_9$[20] with a B/Ge ratio of 4/1, in which B_3O_7 or B_4O_9 BBUs combined with GeO_4 by sharing vertices of oxygen atoms to form B-Ge-O connection mode. BO_4 and RO_4 structural motif are found in low polymer borosilicate $LaBRO_5$[32, 33] with a B/Si ratio of 1, and they form B-O-R six-membered ring formed by sharing vertices of oxygen atoms. While, in R-riched case, the basic R-O units is of a chain or a cluster instead of a ring, and the neighbour R-O chains or clusters share terminal O atoms with BO_4 groups and cations to form a 3D framework, typical examples as $Li_4B_4Si_8O_{24}$[34] and $KBGe_2O_6$[22].

Recently, only tetrahedral basic building units (BBUs) contained materials, such as BPO_4, $LiBGeO_4$ and $Ba_3P_3O_{10}X$ (X = Cl, Br), are reported to have considerable SHG,[1, 29, 35] implying that tetrahedral materials are also to have SHG response comparable with that of compounds contain BO_3 groups. And it is well known that tetrahedral structures possess shorter UV cut-off edge than BO_3, such as the cut-off edges of BPO_4[35] and $LaBGeO_5$[30] are below 134 nm and 193 nm, respectively. These characters make this kind of materials be potential NLO material in deep UV if the SHG response is considerable. In fact, some tetrahedra such as $(AO_4)^{3-}$ (A = P, Si, Ge and V) have been proved to have unnegligible contributions to

SHG response in borate structures $MBPO_5$ (M = Sr, Ba), $LaBRO_5$ (R = Si, Ge) and $Na_3VO_2B_6O_{11}$.[12, 36, 37] However, when and why such tetrahedra will play the important role remains unclear. To address this question, it is necessary to investigate the relation between electronic properties of anionic groups (including tetrahedron and triangle) and optical properties, which is meaningful and vital for exploring and synthesizing various composite NLO materials used in new UV/deep-UV wavelength.

In this work, seven Ge/Si-contained alkaline, alkaline earth and rare earth metal borates with different B-R ratio from B-rich to R-rich ($Rb_2GeB_4O_9$,[20] $RbGeB_3O_7$,[20] $Rb_4Ge_3B_6O_{17}$,[20] $LaBSiO_5$,[33] $LaBGeO_5$,[32] $Li_4B_4Si_8O_{24}$,[34] $KBGe_2O_6$[22]) are studied. The relation between B-R ratio and crystal structures, electronic properties, energy bands, especially optical properties are studied systematically. The SHG-density method is used to character the SHG response of electrons in groups and atoms. The results show that RO_4 and BO_4 also take important role in SHG effect in compounds contain BO_3, particularly the oxygen between tetrahedral. That is because the nonbonding *p* orbitals of bridge oxygens in tetrahedral are closer to Fermi level than the conjugate π orbital in BO_3 after analyzing the PDOS.

2. Computational conditions and theories

2.1. Electronic structures and linear optical properties

The electronic and band structures of ($Rb_2GeB_4O_9$, $RbGeB_3O_7$, $Rb_4Ge_3B_6O_{17}$, $LaBSiO_5$, $LaBGeO_5$, $Li_4B_4Si_8O_{24}$, and $KBGe_2O_6$) are performed by using a plane-wave pseudopotential density functional theory (DFT) implemented in the CASTEP module.[38, 39] For $LaBSiO_5$, $LaBGeO_5$ and $Rb_2GeB_4O_9$, the generalized gradient approximation (GGA) with Perdew–Burke–Ernzerhof (PBE)[40] functional are selected as exchange-correlation potential and ultrasoft pseudopotentials (USP)[41] are used for all chemical elements. The local-density approximation (LDA) for the exchange-correlation potential energy and norm-conserving pseudopotential (NCP)[40, 41] are used for $KBGe_2O_6$, $Li_4B_4Si_8O_{24}$, $Rb_4Ge_3B_6O_{17}$ and $RbGeB_3O_7$. The valence electron configurations for diverse electron orbital pseudopotentials are chosen as Li $2s^1$, K $3s^2$ $3p^6$ $4s^1$, La $5d^1$ $6s^2$, Rb $4s^2$ $4p^6$ $5s^1$, B $2s^2$ $2p^1$, Si $3s^2$ $3p^2$, Ge $4s^2$ $4p^2$, and O $2s^2$ $2p^4$. The plane-wave energy cutoff is set at 830eV for compounds $KBGe_2O_6$, $Li_4B_4Si_8O_{24}$, $Rb_4Ge_3B_6O_{17}$ and $RbGeB_3O_7$; 390 eV for $LaBSiO_5$ and $LaBGeO_5$; 380 eV for $Rb_2GeB_4O_9$. The Monkhorst-Pack k-point is sampled with a separation of less than 0.04 $Å^{-1}$ and other parameters and convergent criteria are set by the default values of the CASTEP code.

A so-called scissors operation[42, 43] is used in evaluation of optical properties. The gap correction Δ is the difference between calculated band gap and experimental one. To determine the refractive index along the principal axes of the seven compounds, the optical permittivity tensor elements are got and the diagonalization transformation is performed.[44] After rotation operation, the linear optical properties of those seven compounds are calculated in the principal dielectric axis coordinate system.

2.2. Methods for calculating non-linear optical properties

At a zero frequency limit, the SHG coefficients are calculated by using the so-called length-gauge formalism derived by Aversa and Sipe.[45] The static second order susceptibilities $\chi_{\alpha\beta\gamma}^{(2)}$ can be written as,[4]

$$\chi_{\alpha\beta\gamma}^{(2)} = \chi_{\alpha\beta\gamma}^{(2)}(\mathrm{VE}) + \chi_{\alpha\beta\gamma}^{(2)}(\mathrm{VH}), \quad (1)$$

Virtual-Electron (VE) can be ascribed as,

$$\chi_{\alpha\beta\gamma}^{(2)}(\mathrm{VE}) = \frac{e^3}{2\hbar m^3}\sum_{vcc'}\int\frac{d^3k}{4\pi^3}P(\alpha\beta\gamma)\,\mathrm{Im}\left[P_{cv}^{\alpha}P_{cc'}^{\beta}P_{c'v}^{\gamma}\right]\left(\frac{1}{\omega_{cv}^3\omega_{vc'}^2}+\frac{2}{\omega_{vc}^4\omega_{c'v}}\right), \quad (2)$$

Virtual-Hole (VH) can be ascribed as,

$$\chi_{\alpha\beta\gamma}^{(2)}(\mathrm{VH}) = \frac{e^3}{2\hbar m^3}\sum_{vv'c}\int\frac{d^3k}{4\pi^3}P(\alpha\beta\gamma)\,\mathrm{Im}\left[P_{vv'}^{\alpha}P_{cv'}^{\beta}P_{cv}^{\gamma}\right]\left(\frac{1}{\omega_{cv}^3\omega_{v'c}^2}+\frac{2}{\omega_{vc}^4\omega_{cv'}}\right), \quad (3)$$

Where α, β, γ are Cartesian components, v and v′ denote valence bands, c and c′ refer to conduction bands, and $P(\alpha\beta\gamma)$ denotes full permutation. The band energy difference and momentum matrix elements are denoted as $\hbar\omega_{ij}$ and P_{ij}^{α}, respectively. Two-band process was proved to be exactly zero which can be neglected in early works.[46]

The band-resolved method[47, 48] is used. By using this method, the effective values individual electronic states in SHG coefficients can be divided into occupied and unoccupied bands, the orbital contributions of total $\chi^{(2)}$ can be calculated. Furthermore, the integral SHG contribution of the corresponding energy region and the contribution of valence bands and conduction bands can be obtained. The SHG-density method[49] is performed by using the effective SHG of each band (occupied and unoccupied) as weighting coefficient (after normalized with total VE or VH $\chi^{(2)}$ value) by summing all the probability densities of occupied or unoccupied states. The SHG density can hence ensure that the quantum states irrelevant to SHG will not be shown in those occupied or unoccupied SHG-density, and the resulting distribution of such density represents a highlight of the origin of SHG.

3. Anionic group frameworks with different B/R ratios

The B-R connection patterns of $KBGe_2O_6$ (ICSD281258), $Li_4B_4Si_8O_{24}$ (ICSD90849), $LaBRO_5$ (ICSD83397, ICSD39262), $Rb_4Ge_3B_6O_{17}$ (ICSD261334), $RbGeB_3O_7$ (ICSD261332), and $Rb_2GeB_4O_9$ (ICSD261333) are shown in Figure 1. It is obvious that the BBUs of B-riched structures $Rb_4Ge_3B_6O_{17}$, $RbGeB_3O_7$ and $Rb_2GeB_4O_9$ are BO_3, BO_4 and RO_4, and the B-O apt to form B_3O_8, B_3O_7 and B_4O_9 rings, respectively. The B-O rings and RO_4 are interlinked through sharing vertices oxygen atoms to form the B-O-R frameworks. For R-riched case with the B/R ratio of 1/2, the BBUs of $KBGe_2O_6$ and $Li_4B_4Si_8O_{24}$ are BO_4 and RO_4, no BO_3 exists. Although the two compounds have the same B/R ratio, the R-O patterns are different. For $KBGe_2O_6$, the $[Ge_2O_7]^{4-}$ dimers formed by condensation of $[GeO_4]^{3-}$ units are linked by topmost O atoms to form a chain along *a* axis. While there are eight different coordination surrounding Si-O groups form four diverse $[SiO_3]_\infty$ chains along *a* axis in $Li_4B_4Si_8O_{24}$, as described in Figure S1 (Supporting Information). The neighbour chains in R-riched $KBGe_2O_6$ and $Li_4B_4Si_8O_{24}$ compounds are all connected by BO_4 groups through sharing vertical oxygens to form the frameworks of anionic groups. The difference of BBUs results in diverse symmetries of these two compounds, those are orthorhombic $P2_12_12_1$ for $KBGe_2O_6$ and monoclinic $P2_1$ for $Li_4B_4Si_8O_{24}$. This may come from the larger radius of K^+ and Ge^{4+} cations, and the different coordination environments of K^+ and Li^+. For the case of B/R ratio of 1, the compounds $LaBRO_5$ show a $[BO_3]_\infty$ spiral chain type formed by BO_4 groups, in which the R atoms are connected with two neighbour BO_4 groups, and neighbour chains are linked by the La^{3+} along *z* axis to form 3D frameworks. Then we get that there is a close relation between the B-R ratio and the BBUs, the B-O groups change from three-coordination to four-coordination along with B-riched to R-riched.

Phys. Chem. Chem. Phys. RSCPublishing

ARTICLE

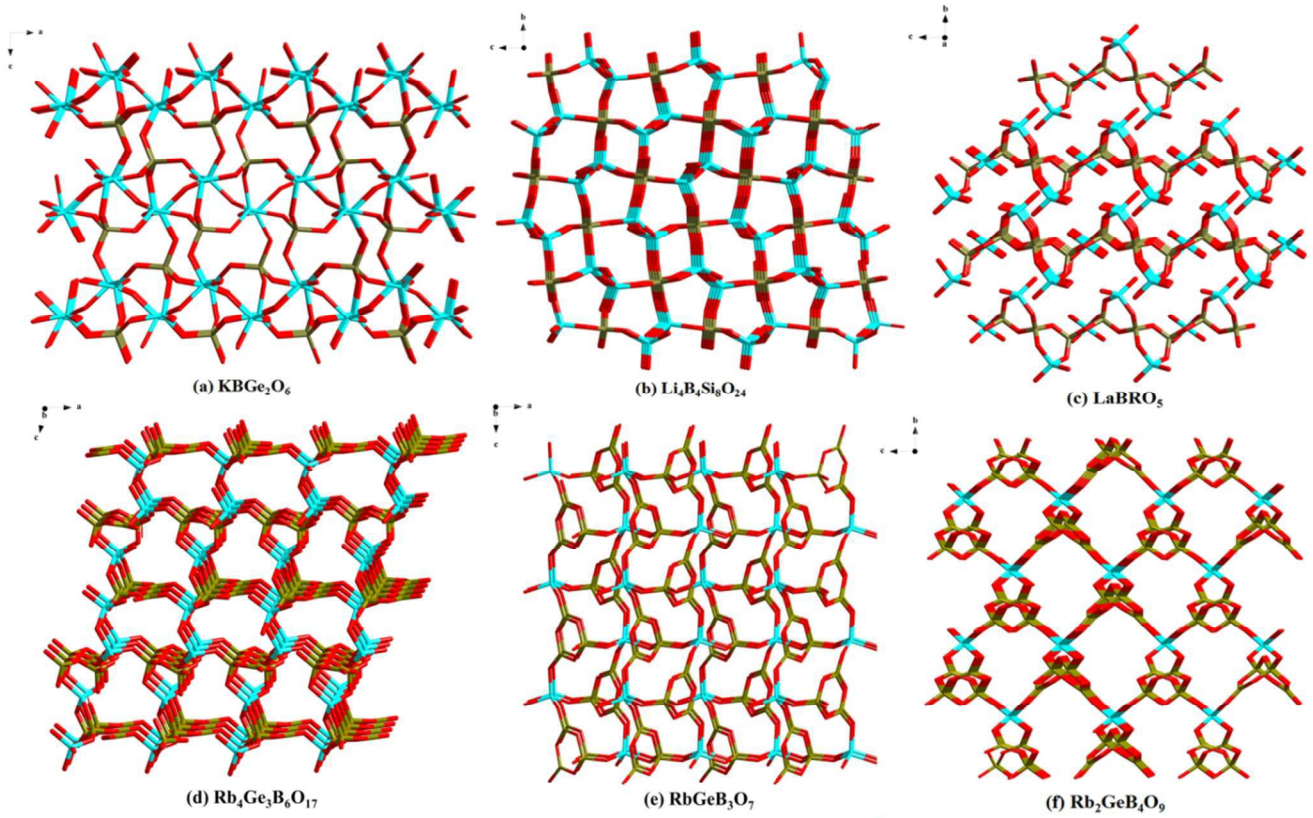

Figure 1. Structures of anionic connection modes for seven compounds. The "green" represents B-O groups, the "blue" represents R-O groups.

4. Results and Discussion

4.1. Electronic structures

The calculated band gaps are shown in Figure S2, $KBGe_2O_6$, $LaBGeO_5$, $Rb_4Ge_3B_6O_{17}$ and $Rb_2GeB_4O_9$ are indirect band gap crystals with the band gaps of 3.769, 4.185, 4.330 and 4.269 eV, respectively. $Li_4B_4Si_8O_{24}$, $LaBSiO_5$ and $RbGeB_3O_7$ are direct band gap crystals with the band gaps of 5.509, 5.158 and 4.770 eV, respectively. The PDOS of $KBGe_2O_6$, $Li_4B_4Si_8O_{24}$, $LaBSiO_5$, $LaBGeO_5$, $Rb_4Ge_3B_6O_{17}$, $RbGeB_3O_7$ and $Rb_2GeB_4O_9$ are demonstrated in Figure S3, from which we can figure out respective contributions of the cations and anionic groups in the near Fermi surface. For the case of B-riched structures $Rb_4Ge_3B_6O_{17}$, $RbGeB_3O_7$ and $Rb_2GeB_4O_9$, the conduction bands are mainly comes from the 4*s* 4*p* of Ge^{4+}, 2*p* of B^{3+}, or *s* 4*p* of Rb^+ and 2*p* of O^{2-}. For R-riched structures $KBGe_2O_6$ or $Li_4B_4Si_8O_{24}$, the *p* of K^+ or 2*s* of Li^+, 4*s* 4*p* of Ge^{4+} or 3*s*, 3*p* of Si^{4+} and 2*p* of O^{2-} makes the main contribution to the bottom of conduction bands. At the top of valence bands in the seven studied compounds, the dominating positions are all occupied by 2*p* orbital of O^{2-}. Generally speaking, for the seven compounds discussed above, the interaction of K^+, Li^+, Rb^+ and La^{3+} cations and the 2*p* orbital of O^{2-} control the near Fermi level. Furthermore, one can get that the orbitals of B and R have changed based on different B-R ratios at the top of valence band.

4.2. Origin of SHG response

Both GW and hybrid functions have been adopted to study the band structures of nonlinear optic crystals,[23, 24, 50] but usually the DFT will underestimate the band gap comparing the experimental value. The scissors operation is used to calculate the optical properties. For the seven studied compounds, the scissors operators are chose as difference between calculated band gap and experimental one or PBE0 results, that is 2.301 eV for $KBGe_2O_6$, 2.619 eV for $Li_4B_4Si_8O_{24}$, 2.375 eV for $LaBSiO_5$, 2.415 eV for $LaBGeO_5$, 1.09 eV for $Rb_4Ge_3B_6O_{17}$, 2.149 eV for $RbGeB_3O_7$ and 1.271 eV for $Rb_2GeB_4O_9$. After the scissors operator, the calculated linear and non-linear optical properties of the seven compounds are shown in Table 1, where the calculated efficient tensors are in good agreement with the SHG response in experiments. In this table, we can see that the larger B/R ratio tends to have a stronger SHG response. According to earlier works on the origin of birefringence

values[51] and SHG response,[44, 52] the BO_3 maybe the main source of both the large birefringence and the SHG response.

Table 1. Experiment and calculated linear and non-linear optical properties.

Compounds	Space group	Experiment band gap	Calculated band gap	Calculated SHG coefficients (pm/V)	Experiment powder SHG response	Calculated birefringence
$KBGe_2O_6$	$P2_12_12_1$	---	3.77 eV	d_{14} = -0.340 (0.87 KDP)	---	0.0050
$Li_4B_4Si_8O_{24}$	$P2_1$	---	5.51 eV	d_{14} = -0.017, d_{16} = -0.012, d_{22} = 0.025, d_{23} = 0.028 (0.07 KDP)	---	0.0083
$LaBSiO_5$	$P3_1$	---	5.16 eV	d_{11} = 0.027, d_{15} = 0.002, d_{22} = -0.385 (0.99 KDP), d_{33} = -0.029	≈1 KDP[36]	0.015
$LaBGeO_5$	$P3_1$	6.41 eV	4.19 eV	d_{11} = 0.142, d_{15} = 0.236, d_{22} = -0.179, d_{33} = -0.310 (0.79 KDP)	0.33 KDP[29]	0.034
$Rb_4B_6Ge_3O_{17}$	Cc	5.42 eV	4.33 eV	d_{15} = -0.634 (1.63 KDP), d_{24} = 0.390, d_{33} = 0.467	1.3 KDP[20]	0.0178
$RbGeB_3O_7$	$Pna2_1$	5.58 eV	4.77 eV	d_{15} = 0.443, d_{24} = 0.694, d_{33} = -0.95 (2.44 KDP)	1.3 KDP[20]	0.0210
$Rb_2GeB_4O_9$	$P2_1$	5.54 eV	4.27 eV	d_{16} = 0.232, d_{14} = -0.864 (2.22 KDP), d_{22} = 0.056, d_{23} = -0.173	2.0 KDP[20]	0.0227

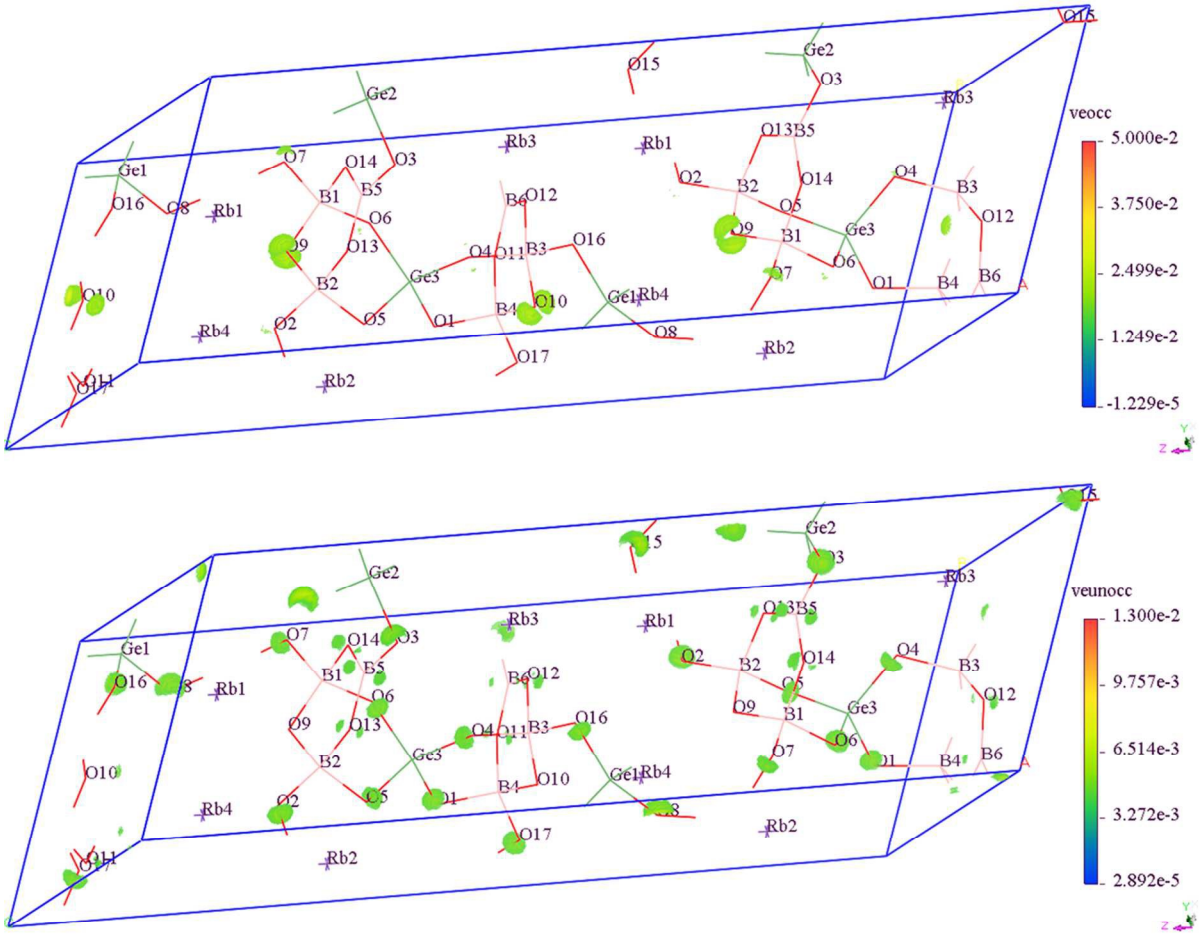

(a) $Rb_4Ge_3B_6O_{17}$

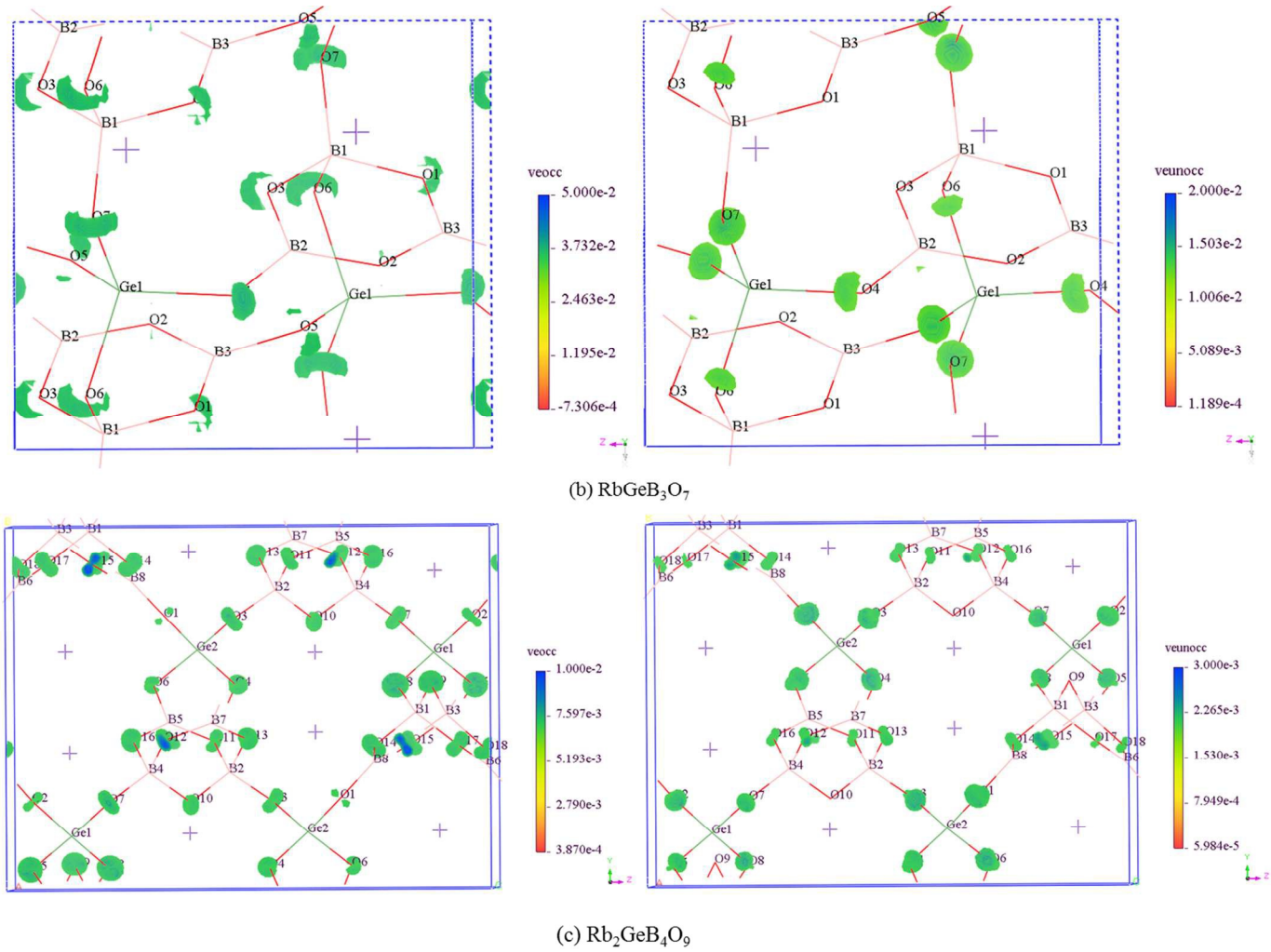

Figure 2. SHG densities of $Rb_4Ge_3B_6O_{17}$, $RbGeB_3O_7$ and $Rb_2GeB_4O_9$. The rainbow represents actives of the veocc state and veunocc state SHG.

In this work, the SHG-density method is employed to analyze the electrons states in three B-riched compounds $Rb_4Ge_3B_6O_{17}$, $RbGeB_3O_7$ and $Rb_2GeB_4O_9$ to study the mechanism of SHG response. The virtual-electron (VE) contributions to the total SHG coefficients are obtained by using the band-resolve method, those are 74.63% (d_{15}), 94.06% (d_{33}) and 86.00% (d_{14}) for $Rb_4Ge_3B_6O_{17}$, $RbGeB_3O_7$ and $Rb_2GeB_4O_9$, respectively. For compound $Rb_4Ge_3B_6O_{17}$, the occupied state of VE is occupied by bridging oxygen O9 and O10, which are the bridging oxygens of two neighbours BO_4 (show in Figure 2). The unoccupied state of VE is taken up by BO_3 groups and the bridging oxygens of GeO_4 and BO_4 (Figure 2a). For $Rb_4Ge_3B_6O_{17}$, the nonbonding 2*p* orbital of bridging oxygens of GeO_4 and BO_4 or BO_3 instead of that in π-conjugation configuration BO_3 groups (Figure 2b) have a considerable contribution to SHG. For the case of $Rb_2GeB_4O_9$, the contributions of SHG are come from BO_3, BO_4 and GeO_4 as shown in Figure 2c. That is to say, the π-conjugation configuration BO_3 group is not the only contributor to SHG response in B-riched structures, especially in $RbGeB_3O_7$. Why the tetrahedral such as BO_4, SiO_4 or GeO_4 do significant contribution to SHG response? To make clear these questions, we have analysed the electron states in the near Fermi surface.

The PDOS of B, Si and Ge are shown in Figure 3 from which one can see that along with the R riched case changing to the B riched one, the state percentage of B-*p* orbital at the top of valence bands tend to grow. The larger percentage of B-*p* orbital indicates that, in the region of -5 ~ 0 eV, the interaction between B/R and O has changed as the variety of B/R ratio. That is to say, the contributor to the SHG response maybe changed with the B/R ratio. From Table 1 we get that for B-riched compounds $Rb_4Ge_3B_6O_{17}$, $RbGeB_3O_7$ and $Rb_2GeB_4O_9$, the SHG coefficients are obviously larger than that of R-riched ones of $KBGe_2O_6$ and $Li_4B_4Si_8O_{24}$. Figure 2 shows the obvious SHG densities of BO_4 or RO_4 tetrahedra, implies the π-conjugation configuration BO_3 is not the only contributor to SHG response, especially in compounds of $Rb_4Ge_3B_6O_{17}$ and $RbGeB_3O_7$.

The PDOS of O atoms for $Rb_4Ge_3B_6O_{17}$ is shown Figure 4a, in which the *p* orbitals of O9 and O10 (the bridging oxygens of two neighbour BO_4 groups) occupy the valence-band maximum, means that O9 and O10 do contribution to SHG response. For $RbGeB_3O_7$ the PDOS of B, O and Ge corresponding to the integral of VE+VH, are given in Figure 4b. The integral of band-resolved $\chi^{(2)}$ increases, corresponding to positive contributions to SHG. One can get that, the *p* orbitals of O1 and O3 (the bridging oxygen of BO_4 and BO_3), O4 and O5 (the bridging oxygen of GeO_4 and BO_3), O6 and O7 (the bridging oxygen of BO_4 and GeO_4), except O2 (the bridging oxygen of two neighbour BO_3 groups), occupies the main region within -1.30 eV ~ 0 eV. That is to say, the non-bonding *p* orbitals of

Phys. Chem. Chem. Phys. RSCPublishing

ARTICLE

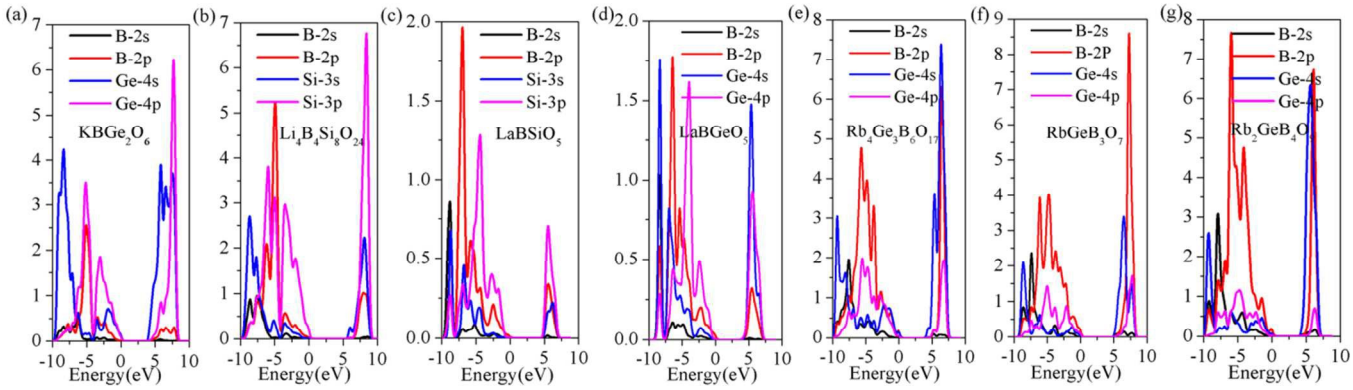

Figure 3. PDOS of B and R (R = Si, Ge) for the seven structures.

bridging oxygens occupy the valence-band maximum, which leads to the SHG response of RO_4. Why the conjugate π orbital in BO_3 have not dominates the top of valence band as previously expected?

For plane trigonal BO_3 group, the overlapping *p* orbitals tend to form π bonding and the non-bonding *p* orbitals decrease, especially for two BO_3 groups connected by sharing vertical oxygen. So the valence-band maximum is mainly occupied by non-bonding *p* orbitals of tetrahedra, such as BO_4 or RO_4, which results in that π-conjugation configuration BO_3 group is not the only contributor to SHG, BO_4 and RO_4 make apparent contribution to SHG (as in compounds $RbGeB_3O_7$).

For structures BO_3 connects with BO_4 or RO_4 groups (as in compounds $Rb_4Ge_3B_6O_{17}$ and $Rb_2GeB_4O_9$), the BO_4 and RO_4 along and π-conjugation configuration BO_3 group have equal important contributions to SHG. This implies that, in a structural unit, π-conjugation configuration BO_3 group do contribution to larger SHG, the tetrahedral BO_4 and RO_4 cannot be neglected. Furthermore, it also tells that the connection pattern of anionic group framework is quite important.

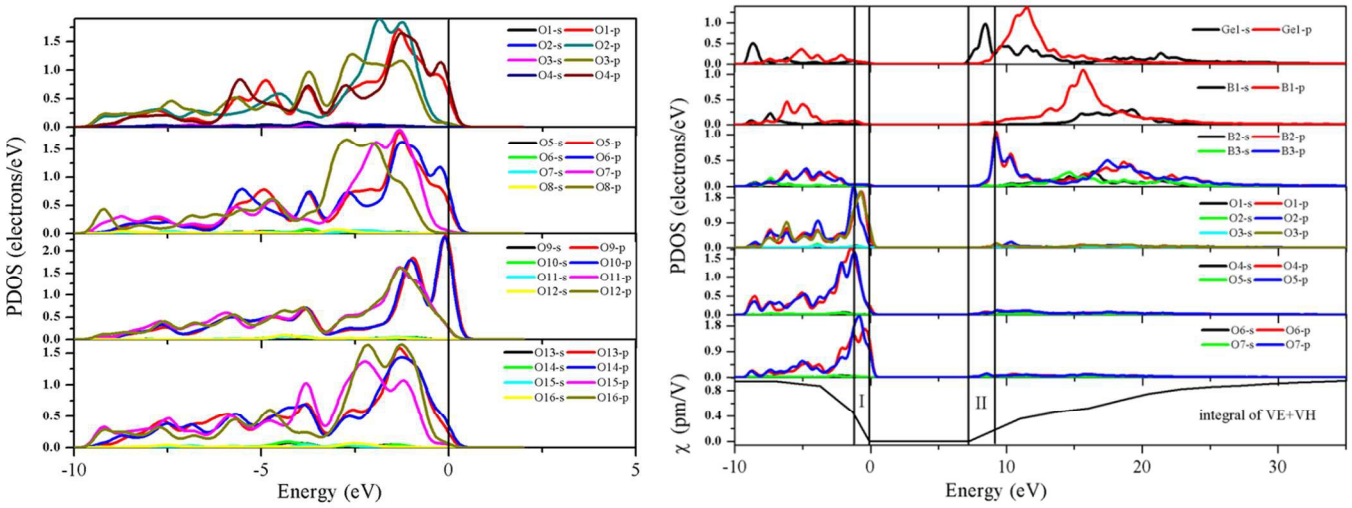

Figure 4. (a) PDOS of O atoms of compounds $Rb_4Ge_3B_6O_{17}$. (b) PDOS of anionic groups B-O and Ge-O and the integral of VE+VH for compound $RbGeB_3O_7$.

5. Conclusions

Using DFT method, band structure, PDOS and SHG density are analyzed to study the influence of the BBUs on linear and non-linear optical properties with different B-R ratios. Based on the SHG density of the seven studied compounds, for B-riched structures $Rb_4Ge_3B_6O_{17}$, $RbGeB_3O_7$ and $Rb_2GeB_4O_9$, BO_3 is not the only contributor to SHG response. This is because valence-band maximum is not occupied only by orbitals of π-conjugation configuration in BO_3 group, the non-bonding *p* orbital of bridging oxygens in BO_4 and RO_4 are closer to Fermi level than that of BO_3 and tetrahedral BO_4 and RO_4 do noticeable contribution to SHG

response. In summary, tetrahedron may do significant contribution to SHG response for Ge/Si-containing borate crystals, which makes it necessary to study this kind of tetrahedral borates and meaningful to design and synthesize NLO material with varied structures.

Acknowledgements

This work is supported by National Basic Research Program of China (Grant No. 2014CB648400), the National Natural Science Foundation of China (Grant Nos, 11265015, 11474353), the Recruitment Program of Global Experts (1000 Talent Plan, Xinjiang Special Program), the Instrument Developing Project of the Chinese Academy of Sciences (Grant No. YZ201349).

Notes and references

[a] School of Physics Science and Technology, Xinjiang University, Urumqi 830046, China;

[b] Xinjiang Technical Institute of Physics & Chemistry, Chinese Academy of Sciences, 40-1 South Beijing Road Urumqi 830011, China;

[c] Department of Physics, Tamkang University, Taipei 25137, Taiwan

† Corresponding Author, email:

zhj@xju.edu.cn.

Electronic Supplementary Information (ESI) available: [Different R-O patterns of $KBGeO_6$ and $Li_4B_4Si_8O_{24}$; Band structures of $KBGe_2O_6$, $Li_4B_4Si_8O_{24}$, $LaBSiO_5$, $LaBGeO_5$, $Rb_4Ge_3B_6O_{17}$, $RbGeB_3O_7$ and $Rb_2GeB_4O_9$; Density of state (DOS) of $KBGe_2O_6$, $Li_4B_4Si_8O_{24}$, $LaBSiO_5$, $LaBGeO_5$, $Rb_4Ge_3B_6O_{17}$, $RbGeB_3O_7$ and $Rb_2GeB_4O_9$.]. See DOI: 10.1039/b000000x/

1. P. Yu, L. M. Wu, L. J. Zhou and L. Chen, *J. Am. Chem. Soc.*, 2014, **136**, 480.
2. H. P. Wu, H. W. Yu, Z. H. Yang, X. L. Hou, X. Su, S. L. Pan, K. R. Poeppelmeier and J. M. Rondinelli, *J. Am. Chem. Soc.*, 2013, **135**, 4215.
3. P. Becker, *Adv. Mater.*, 1998, **10**, 979.
4. J. Lin, M. H. Lee, Z. P. Liu, C. T. Chen and C. J. Pickard, *Phys. Rev. B*, 1999, **60**, 13380.
5. C. T. Chen, Y. C. Wu, A. D. Jiang, B. C. Wu, G. M. You, R. K. Li and S. J. Lin, *J. Opt. Soc. Am. B*, 1989, **6**, 616.
6. Y. Mori, I. Kuroda, S. Nakajima, T. Sasaki and S. Nakai, *Appl. Phys. Lett.*, 1995, **67**, 1818.
7. H. Zhang, M. Zhang, S. L. Pan, X. Y. Dong, Z. H. Yang, X. L. Hou, Z. Wang, K. B. Chang and K. R. Poeppelmeier, *J. Am. Chem. Soc.*, 2015, **137**, 8360.
8. M. C. Chen, L. M. Wu, H. Lin, L. J. Zhou and L. Chen, *J. Am. Chem. Soc.*, 2012, **134**, 6058.
9. H. P. Wu, S. L. Pan, K. R. Poeppelmeier, H. Y. Li, D. Z. Jia, Z. H. Chen, X. Y. Fan, Y. Yang, J. M. Rondinelli and H. S. Luo, *J. Am. Chem. Soc.*, 2011, **133**, 16317.
10. C. T. Chen, Y. C. Wu and R. K. Li, *Int. Rev. Phys. Chem.*, 2008, **8**, 65.
11. J. L. Song, C. L. Hu, X. Xu, F. Kong and J. G. Mao, *Angew. Chem. Int. Edit.*, 2015, **54**, 3679.
12. X. Su, Z. H. Yang, M. H. Lee, S. L. Pan, Y. Wang, X. Y. Fan, Z. J. Huang and B. B. Zhang, *Phys. Chem. Chem. Phys.*, 2015, **17**, 5338.
13. J. J. Zhang, Z. H. Zhang, W. G. Zhang, Q. X. Zheng, Y. X. Sun, C. Q. Zhang and X. T. Tao, *Chem. Mater.*, 2011, **23**, 3752.
14. H. S. Ra, K. M. Ok and P. S. Halasyamani, *J. Am. Chem. Soc.*, 2003, **125**, 7764.
15. X. Su, Y. Wang, Z. H. Yang, X. C. Huang, S. L. Pan, F. Li and M. H. Lee, *J. Phys. Chem. C*, 2013, **117**, 14149.
16. Y. Z. Huang, L. M. Wu, X. T. Wu, L. H. Li, L. Chen and Y. F. Zhang, *J. Am. Chem. Soc.*, 2010, **132**, 12788.
17. M. M. Li, Y. Dai, X. C. Ma, Z. J. Li and B. B. Huang, *Phys. Chem. Chem. Phys.*, 2015, **17**, 17710.
18. W. J. Yao, R. He, X. Y. Wang, Z. S. Lin and C. T. Chen, *Adv. Opt. Mater.*, 2014, **2**, 411.
19. K. Xu, P. Loiseau and G. Aka, *J. Cryst. Growth.*, 2009, 311, 2508.
20. J. H. Zhang, C. L. Hu, X. Xu, F. Kong and J. G. Mao, *Inorg. Chem.*, 2011, **50**, 1973.
21. F. Kong, H. L. Jiang, T. Hu and J. G. Mao, *Inorg. Chem.*, 2008, **47**, 10611.
22. Z. E. Lin, J. Zhang and G. Y. Yang, *Inorg. Chem.*, 2003, **42**, 1797.
23. V. I. Gavrilenko, R. Q. Wu, M. C. Downer, J. G. Ekerdt, D. Lim and P. Parkinson, *Phys. Rev. B*, 2001, **63**, 165325.
24. D. Lim, M. C. Downer, J. G. Ekerdt, N. Arzate, B. S. Mendoza, V. I. Gavrilenko and R. Q. Wu, *Phys. Rev. Lett.*, 2000, **84**, 3406.
25. J. B. P. T. E. Gier, *Chem. Mater*, 1992, **4**, 1065.
26. X. Xu, C. L. Hu, F. Kong, J. H. Zhang, J. G. Mao and J. Sun, *Inorg. Chem.*, 2013, **52**, 5831.
27. H. P. Wu, H. W. Yu, S. L. Pan, Z. J. Huang, Z. H. Yang, X. Su and K. R. Poeppelmeier, *Angew. Chem. Int. Ed. Engl.*, 2013, **52**, 3406.
28. Y. Takahashi, Y. Benino, T. Fujiwara and T. Komatsu, *J. Appl. Phys.*, 2001, **89**, 5282.
29. Y. Takahashi, Y. Benino, T. Fujiwara and T. Komatsu, *Jpn. J. Appl. Phys.*, 2002, **41**, L1455.
30. Y. Takahashi, Y. Benino, V. Dimitrov and T. Komatsu, *J. Non-Cryst. Solids.*, 1999, **260**, 155.
31. O. A. Gurbanova and E. L. Belokoneva, *Crystallogr. Rep+.*, 2007, **52**, 624.
32. E. L. D. Belokoneva, W. I. F.; Forsyth, J. B.; Knight, K. S. , *J. Phys.: Condens. Matter.*, 1997, 3503.
33. L. S. Chi, H. Y. Chen, H. H. Zhuang and J. S. Huang, *J. Alloy. Compd.*, 1997, **252**, L12.
34. J. B. Parise and T. E. Gier, *Int. J. Inorg. Mater.*, 2000, **2**, 81.
35. Z. H. Li, Z. H. Lin, Y. C. Wu, P. Z. Fu, Z. Z. Wang and C. T. Chen, *Chem. Mater.*, 2004, **16**, 2906.
36. L. P. Li, Q. Jing, Z. H. Yang, X. Su, B.-H. Lei, S. L. Pan, F. F. Zhang and J. Zhang, *J. Appl. Phys.*, 2015, **118**, 113104.
37. B.-H. Lei, Q. Jing, Z. H. Yang, B. B. Zhang and S. L. Pan, *J. Mater. Chem. C*, 2015, **3**, 1557.
38. S. J. Clark, M. D. Segall, C. J. Pickard, P. J. Hasnip, M. J. Probert, K. Refson and M. C. Payne, *Z. Kristallogr.*, 2005, **220**, 567.
39. M. C. t. Bernd G. Pfrommer, Steven G. Louie, Marvin L. Cohen, *J. Comput. Phys.*, 1996, **131**, 231.
40. J. P. Perdew, K. Burke and M. Ernzerhof, *Phys. Rev. Lett.*, 1996, **77**, 3865.
41. D. Vanderbilt, *Phys. Rev. B*, 1990, **41**, 7892.
42. C. S. Wang and B. M. Klein, *Phys. Rev. B*, 1981, **24**, 3417.
43. R. W. Godby, M. Schlüter and L. J. Sham, *Phys. Rev. B*, 1988, **37**, 10159.
44. Q. Jing, X. Y. Dong, Z. H. Yang, S. L. Pan, B. B. Zhang, X. C. Huang and M. W. Chen, *J. Solid. State. Chem.*, 2014, **219**, 138.
45. C. Aversa and J. E. Sipe, *Phys. Rev. B*, 1995, **52**, 14636.
46. B. B. Zhang, M. H. Lee, Z. H. Yang, Q. Jing, S. L. Pan, M. Zhang, H. P. Wu, X. Su and C. S. Li, *Appl. Phys. Lett.*, 2015, **106**, 031906.
47. B. B. Zhang, Z. H. Yang, Y. Yang, M.-H. Lee, S. L. Pan, Q. Jing and X. Su, *J. Mater. Chem. C*, 2014, **2**, 4133.
48. M. H. Lee, C. H. Yang and J. H. Jan, *Phys. Rev. B*, 2004, **70**, 235110.
49. C.-H. Lo, *Master Degree thesis，Tamkang University*, 2005.
50. Z. S. Lin, L. Kang, T. Zheng, R. He, H. Huang and C. T. Chen, *Comp. Mater. Sci.*, 2012, **60**, 99.
51. Q. Bian, Z. H. Yang, L. Y. Dong, S. L. Pan, H. Zhang, H. P. Wu, H. W. Yu, W. W. Zhao and Q. Jing, *J. Phys. Chem. C*, 2014, **118**, 25651.
52. C. T. Chen, G. L. Wang, X. Y. Wang and Z. Y. Xu, *Appl. Phys. B-Lasers. O*, 2009, **97**, 9.